Development of an interatomic potential appropriate for simulation of phase transformations in zirconium

Mikhail I. Mendelev*

Materials and Engineering Physics, Ames Laboratory, Ames, IA, 50011, USA

Graeme J. Ackland

Centre for Science at Extreme Conditions, School of Physics, University of Edinburgh, Edinburgh EH9 3JZ, Scotland, UK

*mendelev@ameslab.gov

In recent years there have been some 30 published studies of molecular dynamics (MD) in Zr primarily of its twinning deformation and response to radiation damage: an application for which its low thermal neutron absorption makes it uniquely suited. Surprisingly, current interatomic potentials used do not capture the unusual structural properties of Zr: high stacking fault energy, anomolous diffusion, melting and phase transformation under temperature and pressure (or alloying). *Ab initio* calculations have shown deficiencies in the description of point defects, both vacancies and interstitials, by existing interatomic potentials, which can now be rectified by refitting. Here, we show how to include calculation of phase transitions self-consistently in fitting and present a potential for Zr which correctly reproduces energetics of our own extended database of *ab initio* configurations and high temperature phase transitions. The potential has an analytic many-body form, making it suitable for existing large-scale MD codes. Since it is impossible to fit simultaneously stacking fault energies and phase stability, we also present a best-fit potential for hcp and its defects.

Molecular dynamics has established itself as the key theoretical tool for understanding how microstructural effects in metals occur at the atomistic level. Modern simulation with millions of atoms can investigate collective phenomena such as melting, phase transitions, plastic deformation and radiation damage. Zirconium is a widely studied material in molecular dynamics and statics (e.g., see Willaime and Massobrio (1989), Morris at al. (1995), Serra and Bacon (1996), Pinsook and Ackland (2000), Bacon and Vitek (2002), Osetsky, Bacon and de Diego (2002), Domain and Legris (2005), Trubitsyn, Dolgusheva and Salamatov (2005)), on account of its practical importance in nuclear reactors and its unusual properties of a temperature-induced phase transition and its plastic deformation by twinning, rather than dislocations.

The key ingredient to molecular dynamics is the interatomic potential which determines the forces on the atom. For metals, the delocalised electrons mean that pairwise additive potentials are inappropriate. There are several forms of empirical many-

body potentials (e.g., see a review in Ackland (2006)), of which the most general is the embedded atom method (EAM) (Daw and Baskes 1984). The total energy in EAM is

$$U = \sum_{i=1}^{N-1} \sum_{j=i+1}^{N} V(r_{ij}) + \sum_{i=1}^{N} F(\rho_i) \ , \qquad (1)$$

where the subscripts i and j label each of the N atoms in the system, $r_{i,j}$ is the separation between atoms i and j, V(r) is a pairwise potential, F(ρ) is the embedding energy function and

$$\rho_i = \sum_j \phi(r_{ij}) \ , \qquad (2)$$

where ϕ(r) is another pairwise potential: the "density function". Creating an EAM potential involves finding optimal functions for V(r), F(ρ) and ϕ(r). The complex dependence of fittable quantities on potential parameters means that this is a highly nonlinear optimization problem.

Selecting the quantities to use in the fitting is crucial to potential performance. The results from three popular Zr potentials: IKV (Igarashi, Khantha and Vitek 1991), AWB (Ackland, Wooding and Bacon 1995) and PM (Pasianot and Monti 1999) are summarized in Table 1, including phase transition and melting temperatures for bcc, fcc and hcp phases determined using the co-existence approach (Morris at al. 1994). In this method the simulation is set up with two coexisting phases (e.g. bcc and melt) close to the transition temperature. An NVE-ensemble molecular dynamics simulation with (~15,000 atoms) is run. As the solid-liquid interface moves, latent heat causes a change in the simulation temperature. Provided the equilibrated structure includes both phases, the temperature and pressure of the system will lie on the melting curve. By changing the energy, and using the Clausius-Clapeyron equation, the zero pressure melting temperature can be determined. The simulation is then rerun with incremental changes to the potential parameters. The bcc-hcp transition is suppressed in NVE, so both bcc and hcp single crystals can coexist with the melt, and we can calculate separate melting temperatures for each. The coexistence method proved unsatisfactory for directly determining the hcp-bcc transition temperature, since a single supercell cannot be compatible with two different crystal structures. However the transition temperature can be calculated from the melting data using the Gibbs-Helmholtz relation (Sun at. al. 2006):

$$\int_{T^{hcp\to bcc}}^{T_m^{bcc}} \frac{\Delta E^{hcp\to bcc}}{T^2} dT + \int_{T_m^{bcc}}^{T_m^{hcp}} \frac{\Delta E_m^{hcp}}{T^2} dT = 0 \, , \qquad (3)$$

where the latent heats of the hcp-bcc and hcp melting transitions ($\Delta E^{hcp\to bcc}(T)$ and $\Delta E_m^{hcp}(T)$) are directly determined from the molecular dynamics.

The IKV potential gives rather poor values for unfitted properties, especially interstitial formation energies and thermal expansion, which is so high that the liquid density is 21% smaller than the experimental value. It predicts an hcp-bcc transition but gives the wrong sign for the change in volume. The AWB potential gives reasonable predictions for most other properties except for the phase transformation energies: hcp is

stable up to the melting temperature. Obviously, this deficiency is crucial for using this potential for the simulation of the solid-liquid interface properties and phase transformation in Zr. The PM potential was fitted to the same T=0 crystal properties as the AWB potential, and to exactly reproduce the universal binding energy relation (Rose at. al. 1984) which helps to interpolate between interatomic separations in equilibrium crystals at T=0 and incorporate information about small atomic separations. Table 1 demonstrates that this additional fitting provides no significant improvement in other quantities.

In order to develop those potentials, fitting data for zero-temperature configurations with fixed positions were used, since these are easy to calculate. For most applications energy differences and defect symmetries of relaxed structures are the most relevant quantities. Consequently, in the present work, a self consistent, iterative fitting method is employed. A trial potential is fitted to target structures and energies, the structure is relaxed with this potential, and then the new set of relaxed structures are used to refit the potential. These structures can be ensemble averages, enabling phase transition temperature and liquid structure data to be fitted exactly. Ultimately, this process leads to a potential which gives the correct relaxed and finite temperature properties.

We first test the method by fitting the semi-empirical potential to a pair correlation function (PCF) obtained from an X-ray diffraction experiment (Kelton at. al. 2006) using the Born-Green-Bogoliubov (BGB) equation (Mendelev and Srolovitz, 2002 and Mendelev at. al. 2003). This method incorporates data for all interatomic spacings, including short-ranged ones. We took the AWB potential as a starting potential, and refitted the pairwise potential and embedding energy function to the PCF. The resulting potential (#1 in Table 1) is in excellent agreement with the X-ray diffraction data, it gives slightly poorer reproduction of those quantities fitted by the AWB potential (top eight rows in Table), and similarly results for other properties. This demonstrates that the method proposed in (Mendelev and Srolovitz, 2002) is capable of reproducing of experimental diffraction data. However, the predicted melting temperature is more than 400 K below than experimental value. Although it was not fitted, the #1 potential predicts the hcp-bcc transition and negative change in volume upon this transition although its temperature is well below the experimental value.

The deficiency of all the potentials discussed above to properly predict the phase transformation properties shows that these data must be explicitly included in the fitting procedure. The method to fit the melting point data proposed in (Sturgeon and Laird 2000) could, in principle, be used to fit the solid-solid phase transformation temperature; however, in practice the transition temperature was deduced from the bcc and hcp melting temperatures (see methods), and so we preferred to fit the hcp melting temperature required to reproduce the hcp-bcc transition temperature. To obtain a new potential (#2), we used potential #1 as the initial approximation, changing only V(r) and $F(\rho)$. Firstly we added to the fitting procedure other target quantities listed in Table 1 with appropriate weightings; refitting to these properties did not dramatically change the liquid structure factor. However, when we also tried to fit the phase transformation data we could not reach a reasonable agreement unless we substantially decreased the weighting of the BGB equation fit. We do not know whether this is associated with the basis functions used for V(r), $\phi(r)$ and $F(\rho)$, the cut-off radii, accuracy of the X-ray PCF

or just that an EAM potential is too simplified to reproduce all properties of a real metal. It should be also noted that the agreement with the neutron diffraction data (Schenk at. al. 2002) (which were not used in the fitting procedure) is quite satisfactory as can be seen from Fig. 1.

The complete description of potential #2 is given in Table 2. Table 1 shows that it provides similar agreement with the target T=0 crystal properties as the AWB and PM potentials, but also reproduces the hcp-bcc transformation and melting temperatures, their latent heat and volume changes. This contrasts with, the AWB and PM potentials, which have melting temperatures below the hcp-bcc transition, and the wrong sign for volume change upon the hcp-bcc phase transformation. Potential #2 provides much better predictions for the interstitial formation energies, phase transformation data and liquid structure data than the IKV potential.

A curiosity in the dynamics of zirconium is the rapid self-diffusion, in particular in the bcc phase. We investigate this issue here, which is of particular relevance to radiation damage. An effective self-diffusivity, D^{eff}, was calculated from an NVT MD run with a single defect, following the mean square displacement (MSD) of atoms as a function of time (see Sun at. al. 2006). Such simulations were undertaken at several temperatures (the lattice parameters were adjusted according to temperature) and the resulting values of D^{eff} are shown on an Arrhenius plot in Fig. 2. Since the defect concentration was constant the temperature dependence of D^{eff} is determined solely by the defect migration energy (except of the "perfect" bcc case discussed below). Table 3 summarizes our main results for self-diffusion in Zr. For hcp we examined vacancy, divacancy and interstitial mechanisms. Although the divacancy makes no significant contribution, the extremely low interstitial migration energy means that thermal interstitials can make a significant contribution to self-diffusion. In the bcc phase we investigated vacancy, interstitial and defect-free samples. In the case of samples with vacancies, we obtained results close to reported in Mikhin and Osetsky (1993). In the case of the defect-free samples, we found evidence of an intrinsic diffusion mechanism. Figure 3 shows the evolution of the MSD for "perfect" bcc, showing regions of no diffusion interspersed with rapid diffusion between the creation and annihilation of the intrinsic defect. This intrinsic diffusion mechanism is responsible for the deviations from linearity on the temperature dependence of the effective diffusivity at high temperatures (see Fig. 2).

Examination of Table 1 shows that neither previous potentials nor our #1 and #2 are capable of reproducing the first principles data on the defect formation energy in hcp Zr. The most crucial disadvantages of all potentials are the low basal stacking fault formation energy and the fact that the prism stacking fault formation energy is higher than that for basal stacking fault. As we mentioned above it is difficult to simultaneously reproduce T=0 properties, phase transformation and liquid structure data, and it is impossible to fit basal stacking fault energy and hcp-fcc difference independently in a short-ranged potential. However, an EAM potential can be constructed also reproduce the defect formation energies in hcp Zr. In order to develop this potential (#3) we excluded phase transformation data from the fitting procedure but included the first principles data on the interstitial and stacking fault defect formation energies. As can be seen from Table 1, the ratio of the hcp-fcc energy difference to the basal stacking fault formation energy for all potentials is about 4.2 $Å^2$ while the same ratio calculated from target values is 2.6

Å^2: an EAM potential consisting of smooth functions can reproduce only one of these quantities. Therefore, we also decreased the weighting of the hcp-fcc energy difference. The parameters of potential #3 are presented in Table 2. As can be seen from Table 1, this potential indeed well reproduces the interstitial and stacking fault formation energies but provides rather poor predictions for the phase transformation properties.

In summary, we have derived an interatomic potential for Zr (#2) which properly describes the hcp-bcc phase transition and liquid structure data. As a first test, we have applied the potential to study self-diffusion in hcp and bcc, finding that the anomalously high diffusivity is associated with self-interstitial migration in hcp, and intrinsic defect formation in bcc. While this potential provides a reasonable description of the defect properties crucial to radiation damage simulation, we also developed another potential (#3) which is more suitable if the hcp Zr is the only object of the simulation.

Acknowledgements
The authors thank R.C. Pasianot, D.J. Sordelet, M.J. Kramer, J.R. Morris and B.S. Bokstein for helpful discussions. The Ames Laboratory is operated by the U.S. Department of Energy (DOE) by Iowa State University under Contract No. W-7405-ENG-82. MIM was supported by the Office of Basic Energy Sciences of US DOE, GJA by EPSRC under grant S81186 and the EU under the PERFECT grant.

References:

Ackland G.J. 2006, *J. Nucl.Mater.* **351**, 20.
Ackland G.J., Wooding S.J. and Bacon D.J., 1995, *Phil. Mag. A* **71**, 553.
Arsentev P.P. 1976, *Metallicheskie rasplavy i ikh svoistva* (Moscow: Metallurgia) (in Russian).
Bacon D.J. and Vitek V., 2002, *Metall. Mater. Trans. A* **33**, 721.
Daw M.S. and Baskes M.I., 1984, *Phys. Rev. B* **29**, 6443.
Domain C., 2006, *J. Nuclear Materials* **351**, 1.
Domain C. and Legris A., 2005, *Phil.Mag. A* **85**, 569.
Efimov A.I., Belorukova L.P., Vasilkova I.V. and Chechev V.P., 1983, *Svoistva Neorganicheskih Soedinenii (*Leningrad: Himiia) (in Russian)
Hood G.M., Zou H., Schultz R.J., Matsuura N., Roy J.A. and Jackman J.A., 1997, *Defect and Diffusion Forum* **143-147**, 49.
Igarashi M., Khantha M. and Vitek V., 1991 *Phil. Mag. B* **63**, 603.
Kelton K.F., 2006, Private Communication; Kelton K.F., Gangopadhyay A.K., Kim T.H. and Lee G.W., 2006, J. Non-Cryst. Solids, in press.
Kittel C., 1986, *Introduction to Solid State Physics*, (NY: Wiley)
Lundy T.S., Federer J.I., Pawel R.E. and Winslow F.R., 1965, *in Diffusion in body-centered cubic metals* (Metals Park, Ohio, American Society for Metals)
Mendelev M.I. and Srolovitz D.J. 2002, *Phys. Rev. B* **66**, 014205.
Mendelev M.I., Han S., Srolovitz D.J., Ackland G.J., Sun D.Y. and Asta M., 2003, *Phil. Mag. A*, **83**, 3977.
Mikhin A.G. and Osetsky Yu.N., 1993, *J. Phys.: Condens. Matter* **5**, 9121.
Morris J.R., Ye Y.Y., Ho K.M., Chan C.T. and Yoo M.H., 1995, *Phil. Mag. A* 72, 751.
Morris J.R., Wang C.Z., Ho K.M. and Chan C.T., 1994, *Phys Rev B* **49**, 3109
Osetsky Y.N., Bacon D.J. and de Diego N., 2002, *Metall. Mater. Trans. A* **33** 777.
Pasianot R.C. and Monti A.M., 1999, *J. Nuclear Materials* **264**, 198.
Pearson W.B., 1967, *A handbook of lattice spacings and structures of metals* (Pergamon, Oxford).
Pinsook U. and Ackland G.J., 2000, *Phys. Rev. B* **62**, 5427.
Rose J.H., Smith J.R., Guinea F. and Ferrante J., 1984, *Phys. Rev. B* **29**, 2963.
Serra A. and Bacon D.J., 1996, *Phil.Mag. A* **73**, 333.
Schenk T., Holland-Moritz D., Simonet V., Bellissent R. and Herlach D.M., 2002, *Phys. Rev. Lett.* **89**, 075507
Simmons G. and Wang H., 1971, *Single Crystal Elastic Constants: A Handbook* (MITpress; Cambridge, Mass)
Sturgeon J.B. and Laird B.B., 2000, *Phys. Rev. B* **62**, 14720.

Sun D.Y., Mendelev M.I., Becker C.A., Kudin K., Haxhimali T., Asta M., Hoyt J.J., Karma A., and Srolovitz D.J., 2006, *Phys. Rev. B* **73**, 024116.
Touloukian Y.S., 1975, *Thermophysical properties of matter. Thermal Expansion – Metallic Elements and Alloys* (NY: Plenum)
Trubitsyn V.Y., Dolgusheva E.B. and Salamatov E.I., 2005, *Phys. Solid State* **47,** 1797.
Willaime F. and Massobrio C., 1989, *Phys. Rev. Lett.* **63**, 2244.
VASP: the guide cms.mpi.univie.ac.at/vasp/vasp/vasp.html

Table 1. Physical properties calculated for various interatomic potentials[¥]

Property	Target value	AWB	PM	IKV	#1	#2	#3
a (hcp) (Å)	3.232[1]	**3.249**	**3.232**	**3.232**	**3.231**	**3.220**	**3.234**
c (hcp) (Å)	5.182[1]	**5.183**	**5.149**	**5.149**	**5.186**	**5.215**	**5.168**
E_{coh} (eV/atom)	-6.32[2]	**-6.250**	**-6.250**	**-6.250**	**-6.017**	**-6.469**	**-6.635**
C_{11} (hcp, GPa)	155[3]	**160**	**146**	**155**	196	**165**	**147**
C_{12} (hcp, GPa)	67[3]	**76**	**70**	**67**	88	**65**	**69**
C_{44} (hcp, GPa)	36[3]	**36**	**32**	**36**	47	**48**	**44**
C_{13} (hcp, GPa)	65[3]	**70**	**65**	**65**	81	**63**	**74**
C_{33} (hcp, GPa)	172[3]	**174.7**	**164.8**	**173**	212	**180**	**168**
E_f^v (unrelaxed) (hcp, eV)	2.077[4]	**1.817**	**1.780**	**1.830**	1.550	**2.310**	**1.762**
Octahedral interstitial (T=0)	2.84[5]	4.13	2.81	8.01	3.23	3.51	**2.88**
Basal octahedral interstitial (T=0)	2.88[5]	3.98	2.63	9.10	3.02	2.87	**2.90**
Basal crowdion interstitial (T=0)	2.95[5]	3.82	2.56	8.50	3.25	3.35	**2.91**
I_2 basal stacking fault defect energy (meV/Å^2)	12.5[9]	3.3	4.4	1.7	6.3	6.8	**12.4**
Prism stacking fault defect energy (meV/Å^2)	9.1[9]	unstable	10.1	unstable	unstable	23.3	**10.9**
a (fcc) (Å)	4.53[4]	4.571	4.543	4.553	4.557	**4.545**	**4.538**
$\Delta E_{hcp\rightarrow fcc}$ (eV/atom)	0.032[4]	0.013	0.018	0.007	0.028	**0.030**	**0.054**
a (bcc) (Å)	3.57[4]	3.589	3.568	3.644	3.592	**3.562**	**3.576**
$\Delta E_{hcp\rightarrow bcc}$ (eV/atom)	0.071[4]	0.030	0.053	0.111	0.024	**0.052**	**0.103**
C_{11} (bcc, GPa)	82[4]	119	111	56	114	**96**	**50**
C_{12} (bcc, GPa)	93[4]	119	117	118	98	**109**	**94**
C_{44} (bcc, GPa)	29[4]	83	60	113	63	**42**	**50**
$T_{\alpha\rightarrow\beta}$ (K)	1136[6]	2054 > T_m	1211 > T_m	1251	588	**1233**	*1385*
$\Delta H_{\alpha\rightarrow\beta}$ (eV/atom)	0.040[6]	0.054	0.041	0.037	0.019	**0.039**	*0.058*
$\Delta V_{\alpha\rightarrow\beta}/V_\alpha$ (%)	-0.4[7]	+1.3	+1.9	+4.9	-1.5	**-0.8**	*+0.9*
T_m (hcp, K)		1778	1045	1765	1555	**1913**	*1369*
T_m (bcc, K)	2128[6]	1681	950	1887	1692	**2109**	*1358*
T_m (fcc, K)		1750	988	1739	unstable	unstable	unstable
d (liquid, T=2128 K) (atom/nm^3)	39.56[8]	37.19	37.26	31.39	38.55	**40.08**	**39.65**
ΔH_m (eV/atom)	0.151[6]	0.161	0.108	0.103	0.167	**0.179**	0.078
$\Delta V_m/V_s$ (%)	3.9[6]	4.5	3.7	3.4	4.9	**2.6**	1.2

[¥] The properties used in the fitting procedure are printed in bold.

[1] Pearson (1967)

[2] Kittel (1986)

[3] Simmons and Wang (1971)

[4] Target values are taken from ab initio calculations using the plane wave pseudopotential method (VASP). For these calculations we used GGA exchange and correlation and pseudopotentials (VASP) and k-point sets of 27^3 for single-unit cell properties and 128 atoms with 2^3 k-points for the defects, all of which were relaxed with respect to atomic positions. Our ab initio results are in agreement with the experimental data used, and with similar recent ab initio calculations (Domain and Legris 2005).

[5] Domain and Legris (2005)

[9] Domain (2006)

[6] Efimov at. al. (1983)

[7] Touloukian (1975)

[8] Arsentev (1976)

Table 2. Parameters for the analytical form of potentials #2 (suitable for thermodynamics and phase transitions) and #3(suitable for hcp and plasticity)[§]. Potential #1 is simply a starting condition for deriving #2, and so is not given here.

Function	Value	Cutoffs
$V^{\#2}(r)$	$\exp(12.333392307614-10.847321969086\cdot r+4.5733524424508\cdot r^2-0.85266291445935\cdot r^3)$	1.0-2.3
	$-14.261501929757\cdot(3.5-r)^4+15.850036758176\cdot(3.5-r)^5-11.325102264291\cdot(3.5-r)^6$	
	$-4.0971114831366\cdot(3.5-r)^7+3.6739378016909\cdot(3.5-r)^8$	2.3-3.5
	$+1.3066813393823\cdot(6.0-r)^4-0.60542710718094\cdot(6.0-r)^5+1.0055527194350\cdot(6.0-r)^6$	
	$-0.14918186777562\cdot(6.0-r)^7+0.032773112059590\cdot(6.0-r)^8$	2.3-6.0
	$+0.011433120304691\cdot(7.6-r)^4-0.021982172508973\cdot(7.6-r)^{+5}-0.012542439692607\cdot(7.6-r)^6$	
	$+0.025062673874258\cdot(7.6-r)^7-0.0075442887837418\cdot(7.6-r)^8$	2.3-7.6
$V^{\#3}(r)$	$\exp(12.882230038192-12.183850157814\cdot r+5.5998956281737\cdot r^2-1.0915156420318\cdot r^3$	1.0-2.3
	$+8.4670497139946\cdot(3.5-r)^4-46.183472786003\cdot(3.5-r)^5+79.633499844770\cdot(3.5-r)^6-$	
	$64.847634731465E\cdot(3.5-r)^7+19.454623850774\cdot(3.5-r)^8$	2.3-3.5
	$-0.097845860135187\cdot(6.0-r)^4-0.47537134413743\cdot(6.0-r)^5-0.00096806164225329\cdot(6.0-r)^6-$	
	$0.16355187497617\cdot(6.0-r)^7-0.00090914903435333\cdot(6.0-r)^8$	2.3-6.0
	$-0.022038480751134\cdot(7.6-r)^4-0.060955465943384\cdot(7.6-r)^5+0.11573689045653\cdot(7.6-r)^6-$	
	$0.062697675088029\cdot(7.6-r)^7+0.011273545085049\cdot(7.6-r)^8$	2.3-7.6
$\phi^{\#2}(r)=\phi^{\#3}(r)$	$0.77718711248373\cdot(5.6-r)^4$	0-5.6
	$-0.48102928454986\cdot(5.6-r)^5$	0-5.6
	$+0.14501312593993\cdot(5.6-r)^6$	0-5.6
	$-0.021292226813959\cdot(5.6-r)^7$	0-5.6
	$+0.0012209217625670E\cdot(5.6-r)^8$	0-5.6
$F^{\#2}(\rho)$	$-\rho^{1/2}$	0-∞
	$-1.9162462126235\cdot10^{-7}\cdot(\rho-60)^4$	60-∞
	$+4.6418727035037\cdot10^{-7}\cdot(\rho-70)^4$	70-∞
	$+6.6448294272955\cdot10^{-7}\cdot(\rho-80)^4$	80-∞
	$-2.0680252960229\cdot10^{-6}\cdot(\rho-85)^4$	85-∞
	$+1.1387131464983\cdot10^{-6}\cdot(\rho-90)^4$	90-∞
$F^{\#3}(\rho)$	$-\rho^{1/2}$	0-∞
	$+3.2283012597866\cdot10^{-7}\cdot(ro-60)^4$	60-∞
	$-1.1552813894483\cdot10^{-6}\cdot(ro-70)^4$	70-∞
	$+2.3747280268355\cdot10^{-6}\cdot(ro-80)^4$	80-∞
	$-2.0379550826523\cdot10^{-6}\cdot(ro-85)^4$	85-∞
	$+4.9758343293936\cdot10^{-7}\cdot(ro-90)^4$	90-∞

[§] All distances are expressed in Å and energies in eV.

Table 3. The defect formation[¥] and migration energies taken from our MD runs at 1200K (all energies are in eV/atom). The experimentally measured data come from diffusion measurements, and it is assumed that $E_D = E_f+E_m$ of the lowest defect.

Phase	Defect	E_f at T=1200 K	E_m	E_f+E_m	E_D (experiment)
Hcp	vacancy	2.45	1.24	3.69	3.17[1]
	interstitial	3.00	0.13	3.13	
Bcc	vacancy	2.00	0.44	2.44	2.04[2]
	interstitial	2.04	0.11	2.15	
	intrinsic			3.69	

[¥] The defect formation energies were determined as $E=E(N)-NE_p$, where E is the total energy of the model consisting of N atoms and containing 1 defect and E_p is the total energy per atom of perfect crystal at the same temperature. The energies were averaged over 3,000,000 MD steps (~6 ns).

[1] Hood at. al. (1997)

[2] Lundy at. al. (1965)

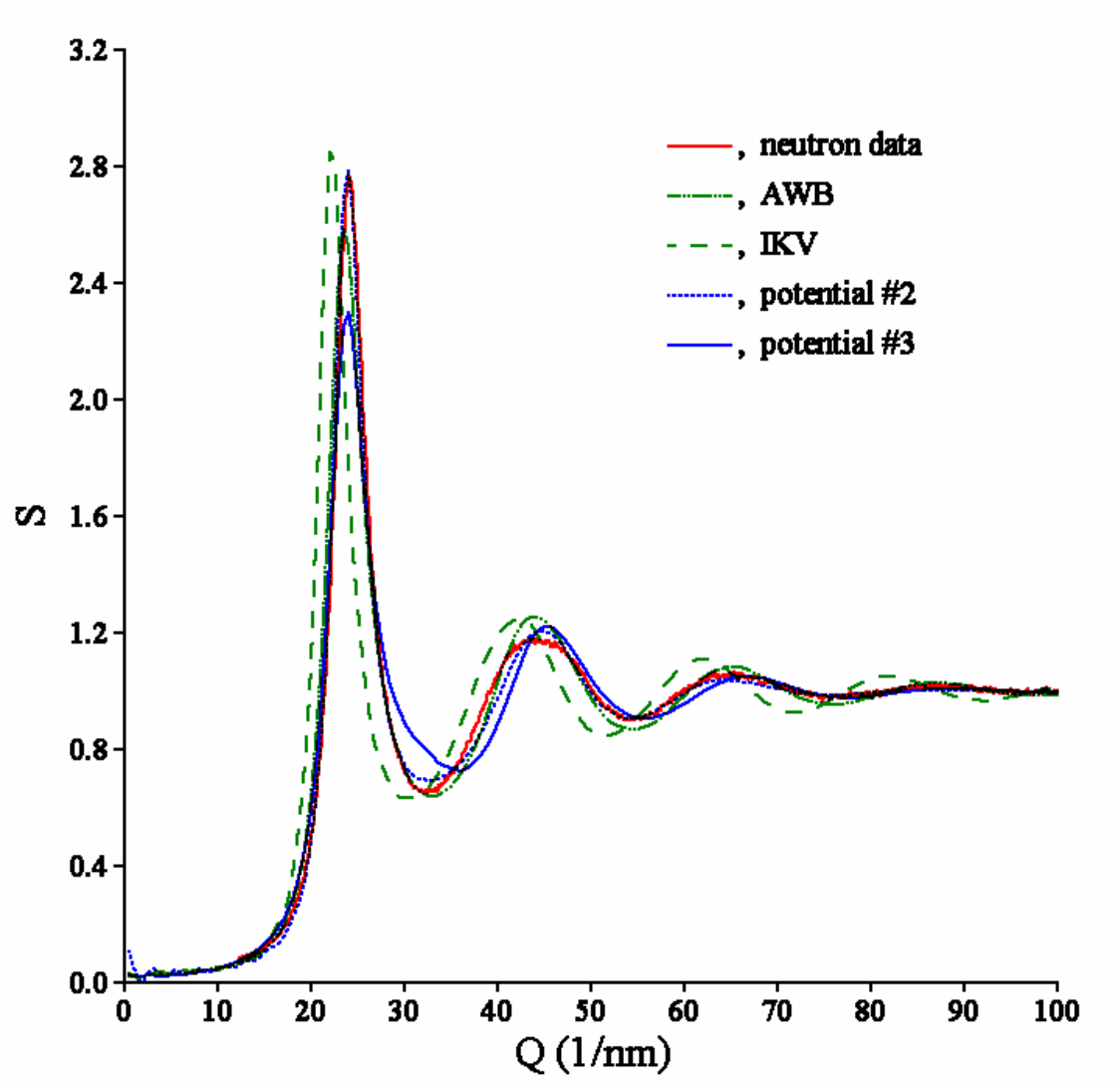

Figure 1. Comparison of calculated and neutron experiment structure factor of liquid Zr at T=2290 K. Calculations were done using three different potentials: IKV and AWB from the literature, and #2 from this work.

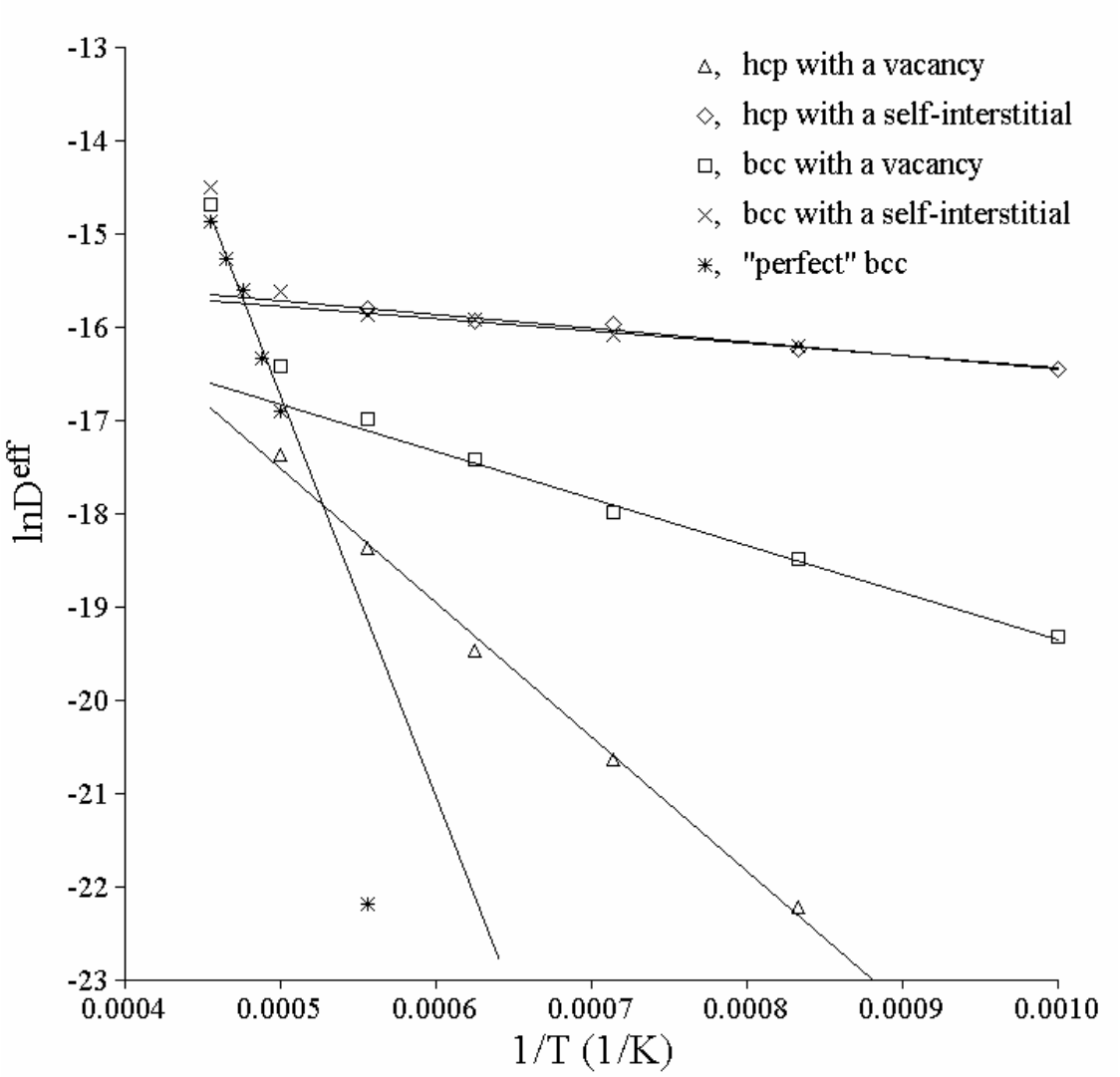

Figure 2. The temperature dependence of the diffusivity calculated under the condition of a fixed defect concentration (see text). The data at two highest temperatures for bcc and the datum at the lowest temperature for "perfect" bcc were excluded from the calculation of the migration energy.

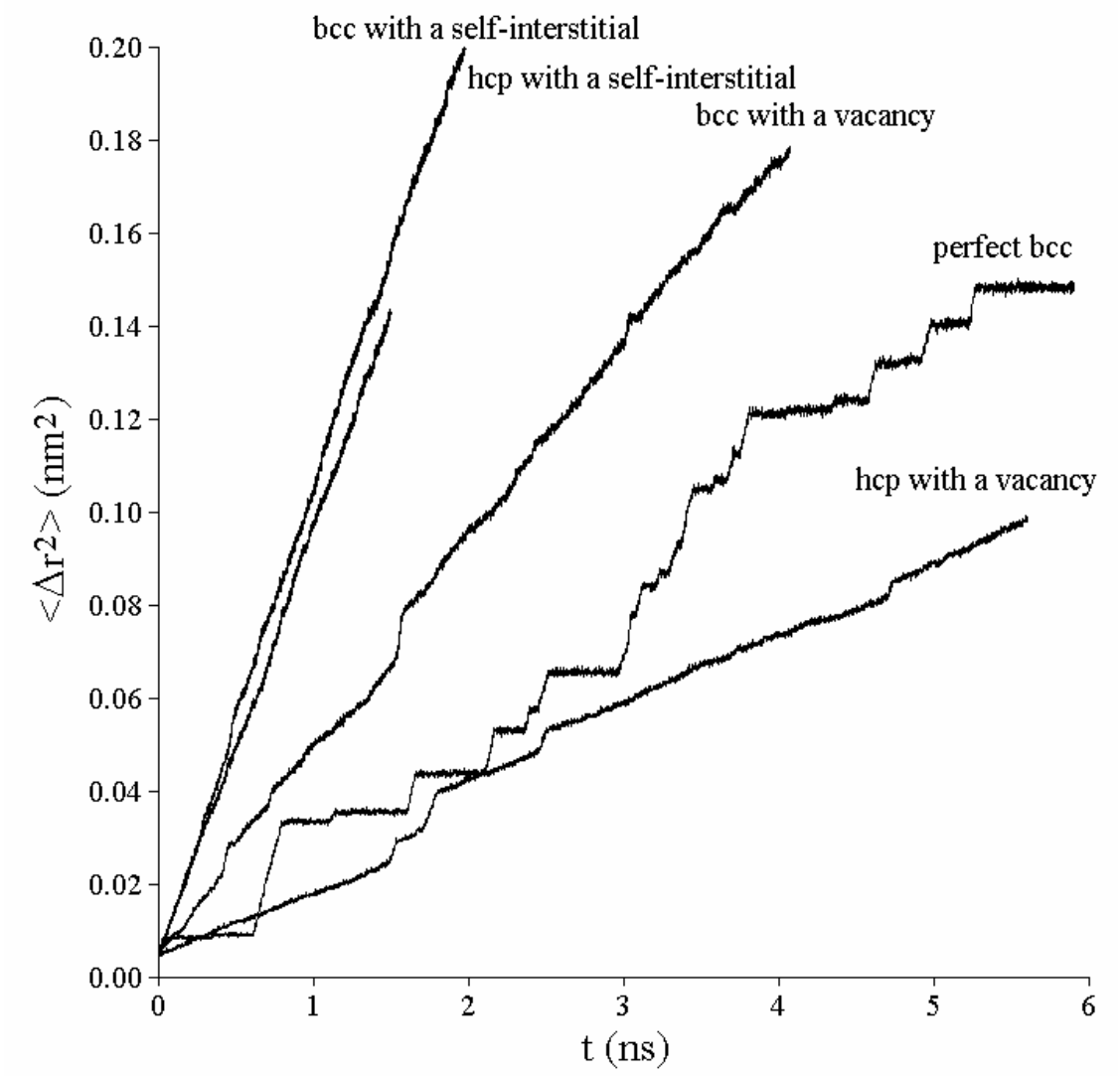

Figure 3. Results deduced from MD simulations with 2688 atoms in the hcp models and 2000 atoms in the bcc models at T=2000 K for several defect types.

Development of an Interatomic Potential Appropriate for Simulation of Phase Transformations in Zirconium M. I. Mendelev* Materials and Engineering Physics, Ames Laboratory, Ames, IA, 50011, USA G.J. Ackland Centre for Science at Extreme Conditions, School of Physics, University of Edinburgh, Edinburgh EH9 3JZ, Scotland, UK *.Â Surprisingly, current interatomic potentials used do not capture the unusual structural properties of Zr: high stacking fault energy, anomolous diffusion, melting and phase transformation under temperature and pressure (or alloying). Ab initio calculations have shown deficiencies in the description of point defects, both vacancies and interstitials, by existing interatomic potentials, which can now be rectified by refitting. Interatomic potential models of course take no explicit account of electronic structure. They cannot therefore be used to model spectroscopic properties, or reactivity (although we note the ReaxFF forcefield [15] attempts to include the description of bond making and breaking). The methods are, however, widely applicable and with current computational resources can be used to simulate large and complex systems.Â These moves will normally involve displacement of a particle but in â€œGrand Canonical Monte Carloâ€ (GCMC) simulation moves also involve creation and deletion of particles with a specified chemical potential. MC simulations are appropriate for calculating thermodynamic properties and they also give valuable information about particle distribution in the simulated system. Department of Physics. Development of interatomic potentials in the Terso-Albe formalism for metal compounds. Oppiaine â€” LÂ¨aroÂ¨amne â€” Subject. Fysik.Â Interatomic potentials are used to describe the motion of the individual atoms in atomistic simula-tions. An accurate treatment of the interatomic forces in a system of atoms requires heavy quantum mechanical calculations, which are not computationally feasible in large-scale simulations. Intera-tomic potentials are computationally more ecient analytical functions used for calculating the potential energy of a system of atoms, allowing simulations of larger systems or longer time scales than in quantum mechanical simulations.